

# Theoretical Assessment of Dinitrogen Fixation on Carbon Atom

Hayoung Song<sup>[a]</sup> and Eunsung Lee<sup>[a, b]\*</sup>

[a] H. Song, Prof. E. Lee  
Department of Chemistry, Pohang University of Science and Technology (POSTECH), Pohang, 37673, Republic of Korea  
E-mail: eslee@postech.ac.kr (E. Lee)

[b] Prof. E. Lee  
Graduate school of artificial intelligence, Pohang University of Science and Technology. Pohang, 37673, Republic of Korea.

Supporting information for this article is given via a link at the end of the document

**Abstract:** Dinitrogen activation in non-metallic systems has received considerable attention in recent years. Herein, we report the theoretical feasibility of N<sub>2</sub> fixation using aminocarbenes (**L**) or their anionic derivatives. The molecular descriptors of **L** and anionic L<sup>-</sup>, which affect the interaction of **L** and anionic L<sup>-</sup> with N<sub>2</sub>, were identified through multiple linear regression analysis. Additionally, the electron flow during C–N bond formation was confirmed by performing intrinsic reaction coordination calculations with intrinsic bond orbital analysis for the reaction of anionic L<sup>-</sup> with N<sub>2</sub>.

Dinitrogen (N<sub>2</sub>) is the most abundant and easily accessible nitrogen source in nature. The synthesis of useful chemicals using N<sub>2</sub>, from NH<sub>3</sub><sup>[1]</sup> to N-containing organic molecules<sup>[2]</sup>, has a long history and is still considered most challenging in chemistry. The development of systems for metal-free N<sub>2</sub> fixation is particularly difficult. Recently, boron-containing organic materials have attracted attention as materials for metal-free N<sub>2</sub> fixation. The fixation and electrocatalytic reduction of N<sub>2</sub> using graphene doped with boron were reported by Zheng et al.<sup>[3]</sup> The Braunschweig group also reported the fixation and reduction of N<sub>2</sub> using organic borylene.<sup>[4]</sup> Zhu et al. reported the theoretical systematic design of frustrated Lewis pairs using a highly Lewis acidic borole as the active site, with N-heterocyclic carbenes (NHCs).<sup>[5]</sup> However, to date, there are no reported examples of N<sub>2</sub> fixation using only carbon active sites.

Persistent aminocarbenes, represented by NHCs, have been utilized for metal-free small-molecule activation. Persistent aminocarbenes successfully react with CO<sub>2</sub>, SO<sub>2</sub>, NO, and N<sub>2</sub>O as well as inert molecules such as H<sub>2</sub> and CO.<sup>[6]</sup> Furthermore, the metal-free catalytic conversion of CO<sup>[7]</sup> over an aminocarbene catalyst was also reported. Considering that CO is isoelectronic with N<sub>2</sub>, aminocarbene can be effectively utilized as the carbon active site for N<sub>2</sub> fixation.

Herein, we report theoretical studies on N<sub>2</sub> fixation on carbon atoms. We explored 20 typical examples of aminocarbene (**L**)<sup>[8]</sup> in five binding modes with N<sub>2</sub> (**Figure 1**). We confirmed that although thermodynamically favored products can be obtained from the reaction of **L** and N<sub>2</sub>, the reaction is not kinetically favored. The thermodynamic and kinetic effects on the interaction between **L** and N<sub>2</sub> were investigated using the molecular descriptor **L**. We

also reported that the anionic L<sup>-</sup> radical can overcome the high activation barrier of **L** in the reaction with N<sub>2</sub>.

First, we attempted to establish possible candidates that could be obtained from the reaction of **L** with N<sub>2</sub>. With the proposal that the reactivity of NHCs can mimic the reactivity of transition metals,<sup>[6a]</sup> we proposed five structures of possible products based on previously reported transition metal–N<sub>2</sub> complexes (**Figure 1**).<sup>[9]</sup> The ligand hapticity of N<sub>2</sub> has been reported for both η<sup>1</sup> and η<sup>2</sup> for transition metal–N<sub>2</sub> complexes. Thus, L(η<sup>1</sup>-N<sub>2</sub>) and L(η<sup>2</sup>-N<sub>2</sub>) were chosen as mononuclear L(N<sub>2</sub>) complexes. Furthermore, referring to the examples of the reported bimetallic N<sub>2</sub> complexes,<sup>[9]</sup> L<sub>2</sub>(μ-η<sup>1</sup>:η<sup>1</sup>-N<sub>2</sub>), L<sub>2</sub>(μ-η<sup>2</sup>:η<sup>2</sup>-N<sub>2</sub>), and L<sub>2</sub>(μ-η<sup>1</sup>:η<sup>2</sup>-N<sub>2</sub>) were also selected as binuclear L<sub>2</sub>(N<sub>2</sub>) complexes. L(η<sup>1</sup>-N<sub>2</sub>) and L(η<sup>2</sup>-N<sub>2</sub>) can be considered as diazoalkane and diazine derivatives, which have been actively used as precursors of transient carbenes. L<sub>2</sub>(μ-η<sup>1</sup>:η<sup>1</sup>-N<sub>2</sub>) can also be considered an azaalkane derivative. Each structure was optimized by Gaussian 16 using the B3LYP functional with the Def2-SVP basis set.

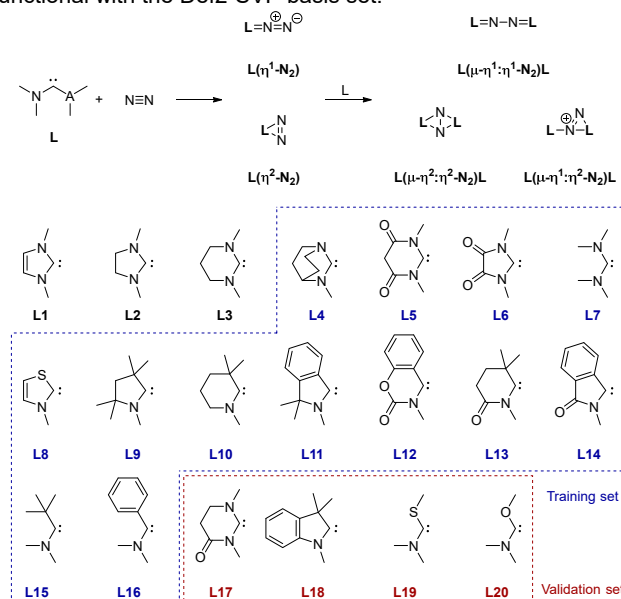


**Figure 1.** Selected training/validation aminocarbene **L** sets on five L–N<sub>2</sub> binding modes.

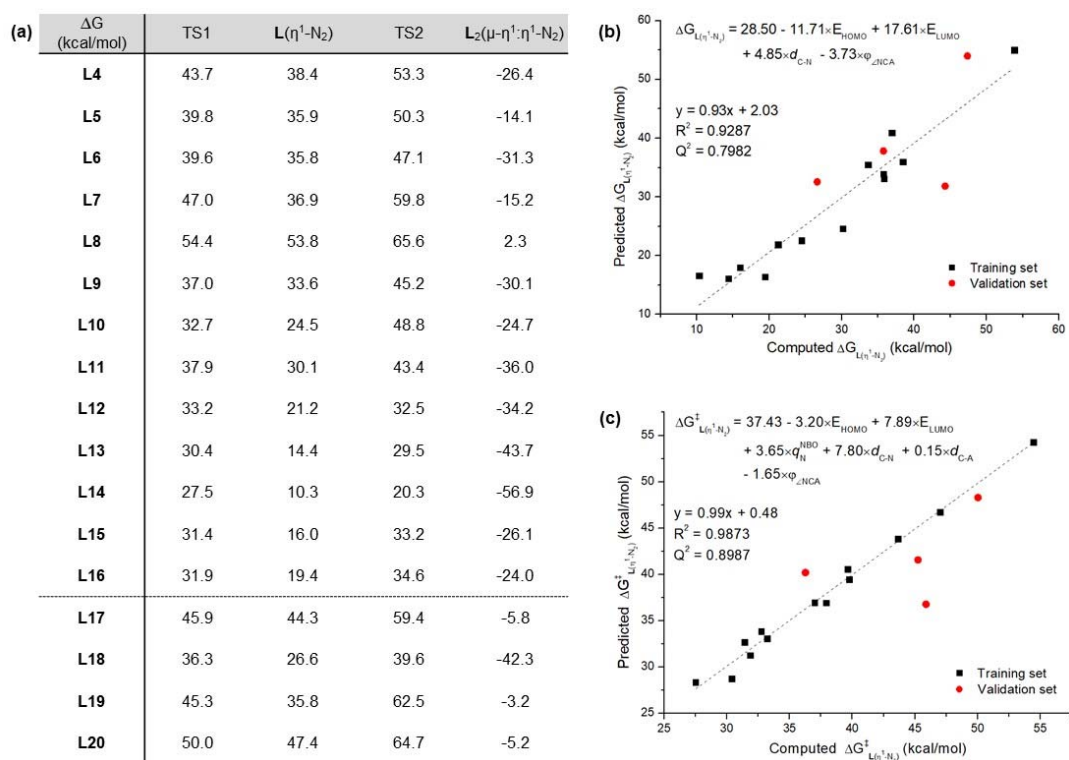


**Figure 2.** (a) Detailed free energies of the formation of  $L-N_2$  complex and its transition states. (b) Comprehensive model of the free energy of  $L(\eta^1-N_2)$  formation. (c) Comprehensive model of the activation barrier of  $L(\eta^1-N_2)$  formation (computed using Gaussian 16 at the B3LYP/Def2-SVP level).

As a result, the formation of  $L(\eta^1-N_2)$ ,  $L(\eta^2-N_2)$ , and  $L_2(\mu-\eta^2:\eta^2-N_2)$  was thermodynamically unfavorable for all **L** (**Figure 2a**). Unfortunately, the structure optimization of  $L_2(\mu-\eta^1:\eta^2-N_2)$  for some **L** failed; however, the formation of other successfully optimized  $L_2(\mu-\eta^1:\eta^2-N_2)$  was thermodynamically unfavorable, except for **L13** and **L14**. The formation of  $L_2(\mu-\eta^1:\eta^1-N_2)$  was thermodynamically preferred for most **L**, except for **L1** to **L3** and **L8**. Therefore, we chose  $L_2(\mu-\eta^1:\eta^1-N_2)$  as a suitable model for  $N_2$  fixation on carbon atoms.

Despite the high thermodynamic stability of  $L_2(\mu-\eta^1:\eta^1-N_2)$ , the real challenge for dinitrogen fixation on carbon atoms is that the formation of intermediate  $L(\eta^1-N_2)$  is kinetically and thermodynamically unfavorable. We confirmed the high activation barrier for the formation of  $L(\eta^1-N_2)$  ( $\Delta G^\ddagger(L(\eta^1-N_2)) = 27\text{--}55$  kcal/mol) between **L4** and **L20** (**Figure 2a**). The activation barrier for the formation of  $L_2(\mu-\eta^1:\eta^1-N_2)$  from  $L(\eta^1-N_2)$  was relatively low ( $\Delta G^\ddagger(L_2(\mu-\eta^1:\eta^1-N_2)) = 10\text{--}27$  kcal/mol).

We identified the correlation of  $\Delta G$  and  $\Delta G^\ddagger$  with the normalized molecular descriptors for **L** through multiple linear regression (MLR) analysis.<sup>[10]</sup> Considering the small size of dinitrogen, steric descriptors, such as  $V_{bur}$  and Sterimol parameters, were omitted from the selection of the molecular descriptor of **L**. We selected the molecular descriptor for MLR analysis using a correlation map to remove multicollinearity of the selected molecular descriptors (**Figures S1** and **S2**).

Because of the strong correlation between  $\Delta G(L(\eta^1-N_2))$  and  $\Delta G^\ddagger(L(\eta^1-N_2))$  ( $R^2 = 0.93$ ), similar models were produced by

performing MLR on selected molecular descriptors with the robustness of the correlations ( $R^2 = 0.92$  for **Figure 2b** and  $R^2 = 0.98$  for **Figure 2c**).  $\Delta G(L(\eta^1-N_2))$  strongly depends on  $E_{HOMO}$  and  $E_{LUMO}$  and weakly on  $d_{C-N}$  and  $\phi_{\perp NCA}$ . Similarly,  $\Delta G^\ddagger(L(\eta^1-N_2))$  depends on  $E_{HOMO}$ ,  $E_{LUMO}$ ,  $q^{NBON}$ ,  $d_{C-N}$ , and  $\phi_{\perp NCA}$  and weakly on  $d_{C-A}$ . Commonly,  $\Delta G(L(\eta^1-N_2))$  and  $\Delta G^\ddagger(L(\eta^1-N_2))$  are more dependent on  $E_{LUMO}$  than on  $E_{HOMO}$ , indicating that the reactivity of **L** with  $N_2$  was more influenced by the Lewis acidity of **L**.

For  $N_2$  fixation using **L** without additional reagents, it is necessary to design an ambiphilic **L** with high HOMO and low LUMO energy levels. However, the low thermal stability<sup>[8e, 11]</sup> of previously reported ambiphilic aminocarbenes is not suitable for overcoming the high activation barrier ( $\Delta G^\ddagger(L(\eta^1-N_2)) > 27$  kcal/mol) for the formation of  $L(\eta^1-N_2)$ .

Instead of designing a new ambiphilic aminocarbene with high thermal stability, we proposed another strategy for  $N_2$  fixation using previously reported **L** to achieve a low activation barrier for  $N_2$  fixation. Low-valent transition metal complexes have received continuous interest as promising catalyst candidates for  $N_2$  fixation and catalytic reduction.<sup>[12]</sup> The high electron density of the low-valence transition metal allows the formation of a stable  $N_2$  complex through strong  $\pi$ -backdonation on the  $N_2$  ligand. We proposed that the aminocarbene derivatives **L**, mimicking the reactivity of transition metals, can form stable  $L(\eta^1-N_2)$  radical anions via one-electron reduction.

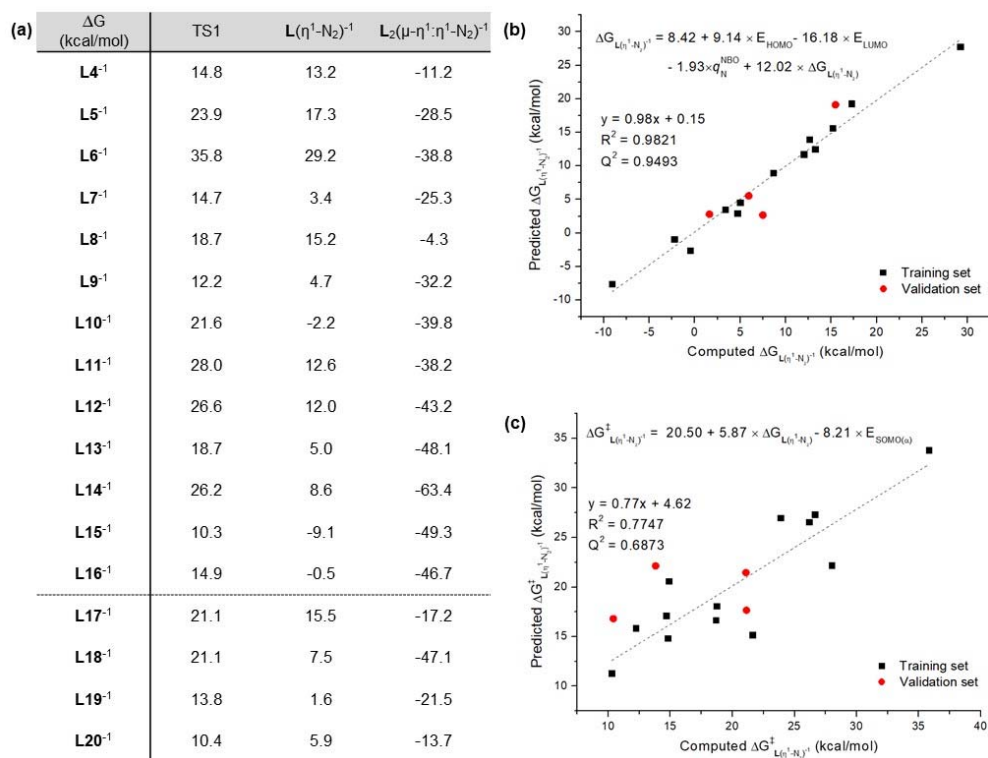


**Figure 3.** (a) Detailed free energies of the formation of the anionic  $L^-N_2$  complex and its transition state. (b) Comprehensive model of the free energy of anionic  $L(\eta^1-N_2)^-$  formation. (c) Comprehensive model of the activation barrier of anionic  $L(\eta^1-N_2)^-$  formation. (computed using Gaussian 16 at the B3LYP/Def2-SVP level)

The structures of anionic  $L^-$ ,  $L(\eta^1-N_2)^-$  and  $L_2(\mu-\eta^1:\eta^1-N_2)^-$  radicals and their transition states were optimized at the B3LYP/Def2-SVP level. The results indicated that the formation of anionic  $L(\eta^1-N_2)^-$  and  $L_2(\mu-\eta^1:\eta^1-N_2)^-$  radicals is thermodynamically more favored than that of neutral  $L(\eta^1-N_2)$  (Figure 3a). The formation of  $L(\eta^1-N_2)$  radical anions was slightly exothermic for **L10**, **L15**, and **L16** (-2.2, -9.1, and -0.5 kcal/mol). Furthermore, we confirmed that the activation barrier of the reaction between the anionic radical derivatives of **L** and  $N_2$  decreased drastically. For example, the free energy of  $L(\eta^1-N_2)$  formation decreased from 33.6 kcal/mol to 4.7 kcal/mol, and its activation barrier also significantly decreased from 37.0 kcal/mol to 12.2 kcal/mol (Figure 4). The activation barrier of **L9** $(\mu-\eta^1:\eta^1-N_2)$  formation was also decreased from 11.6 kcal/mol to 6.8 kcal/mol. However, the activation barrier of  $L(\eta^1-N_2)$  formation for **L6**, **L11**, **L12**, and **L14** radical anions, which are highly ambiphilic aminocarbenes, was not significantly decreased. ( $\Delta\Delta G^\ddagger < 10$  kcal/mol).

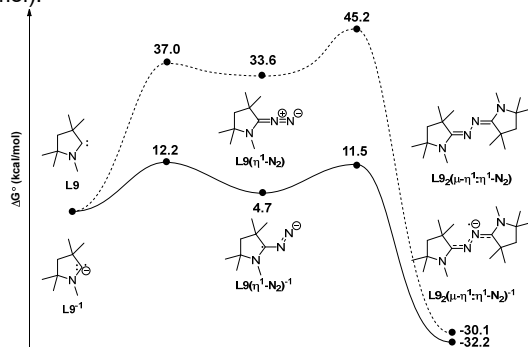


**Figure 4.** Free energy profile of the reaction of **L9** and **L9<sup>-1</sup>** with  $N_2$  as calculated using Gaussian 16 at the B3LYP/Def2-SVP level.

We also performed MLR analysis to determine how the molecular descriptors of **L** affect the free energy and activation barrier of anionic  $L(\eta^1-N_2)^-$  formation. We considered both the molecular descriptors of neutral and anionic  $L^-$ . In addition, the free energy and activation barrier of neutral  $L(\eta^1-N_2)$  formation were considered as additional molecular descriptors. In the removal of multicollinearity using the correlation maps of selected parameters, the molecular descriptors of neutral **L** were selected prior to the molecular descriptors of anionic  $L^-$  (Figure S1).

Interestingly, there is a relatively low correlation between the free energy of anionic  $L(\eta^1-N_2)^-$  formation and its activation barrier ( $R^2 = 0.52$ ), unlike neutral  $L(\eta^1-N_2)$  formation ( $R^2 = 0.93$ ) (Figures S1 and S2). The free energy and activation barrier of the  $L(\eta^1-N_2)$  radical anion were significantly dependent on the free energy of neutral  $L(\eta^1-N_2)$  (Figure 3b and 3c). In addition, the free energy of the  $L(\eta^1-N_2)$  radical anion decreased with decreasing  $E_{HOMO}$  and increasing  $E_{LUMO}$  of neutral **L**. However, the activation barrier of the formation of the  $L(\eta^1-N_2)$  radical anion decreased significantly with increasing  $E_{SOMO(\alpha)}$  of anionic  $L^-$ . This result indicates that the  $SOMO(\alpha)$  of anionic  $L^-$  largely contributes to the reaction of **L** with  $N_2$ .

Intrinsic reaction coordination calculations and intrinsic bond orbital (IBO) analysis<sup>[13]</sup> were performed to confirm the electron flow during C-N bond formation between anionic **L9** and  $N_2$  (Figure 5). In the optimized transition state,  $N_2$  approached the vertical direction of the carbene. Thus,  $\sigma$ -bond formation between the  $\pi^*$  orbital of  $N_2$  and the  $SOMO(\alpha)$  of anionic  $L^-$  occurred preferentially. Thereafter, the new  $\pi$ -bond derived from the HOMO was formed when the other  $\pi^*$  orbital of  $N_2$  and the HOMO of anionic  $L^-$  were sufficiently close.

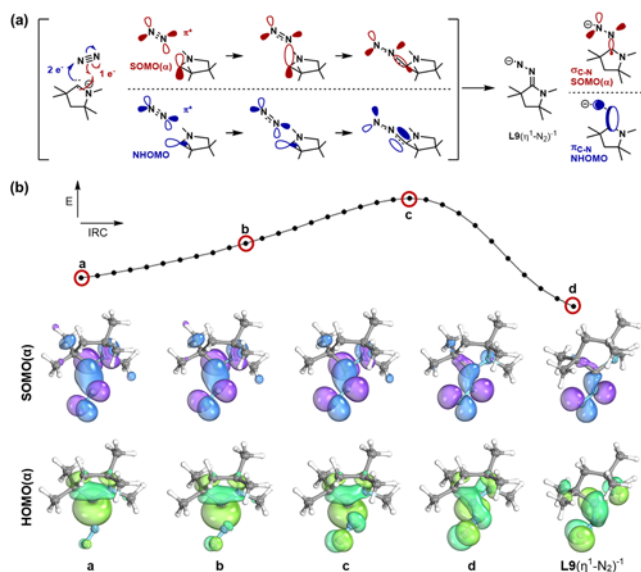


**Figure 5.** Mechanism of electron flow during the reaction between anionic  $L^-$  and  $N_2$  visualized through IBO analysis.

In summary, we confirmed that the reactivity of  $L$  with  $N_2$  was influenced by their HOMO and LUMO energy levels, C–N and C–A bond lengths, bond angles of N–C–A, and nitrogen atom charges. From these results, we discovered that  $N_2$  fixation using the anionic  $L^-$  radical significantly lowers the activation energy of the reaction of  $L$  with  $N_2$  via the interaction between the SOMO( $\alpha$ ) of  $L^-$  and the  $\pi^*$  orbital of  $N_2$ . This study suggested that  $N_2$  fixation on carbon atoms can be achieved through the design of (1) thermodynamically highly stable ambiphilic aminocarbenes or (2) aminocarbenes capable of one-electron reduction, which can serve as an important route for the entry of non-metallic systems.

## Acknowledgements

This work was supported by the National Supercomputing Center with supercomputing resources including technical support (KSC-2019-CRE-0162), and by the National Research Foundation of Korea (NRF-2019R1A2C2010732).

**Keywords:** Dinitrogen, Carbene,  $N_2$  fixation, N-heterocyclic carbene, DFT calculation

- [1] (a) B. M. Hoffman, D. Lukoyanov, Z.-Y. Yang, D. R. Dean, L. C. Seefeldt, *Chem. Rev.* **2014**, *114*, 4041-4062; (b) R. R. Schrock, *Acc. Chem. Res.* **2005**, *38*, 955-962; (c) M. J. Chalkley, T. J. Del Castillo, B. D. Matson, J. P. Roddy, J. C. Peters, *ACS Cent. Sci.* **2017**, *3*, 217-223; (d) Y. Nishibayashi, *Dalton Trans.* **2018**, *47*, 11290-11297.
- [2] (a) M. Mori, *J. Organomet. Chem.* **2004**, *689*, 4210-4227; (b) A. J. Keane, W. S. Farrell, B. L. Yonke, P. Y. Zavalij, L. R. Sita, *Angew. Chem. Int. Ed.* **2015**, *54*, 10220-10224; (c) J. J. Curley, A. F. Cozzolino, C. C. Cummins, *Dalton Trans.* **2011**, *40*, 2429-2432; (d) I. Klopsch, M. Kinauer, M. Finger, C. Würtele, S. Schneider, *Angew. Chem. Int. Ed.* **2016**, *55*, 4786-4789; (e) S. F. McWilliams, D. L. J. Broere, C. J. V. Halliday, S. M. Bhutto, B. Q. Mercado, P. L. Holland, *Nature* **2020**, *584*, 221-226.
- [3] X. Yu, P. Han, Z. Wei, L. Huang, Z. Gu, S. Peng, J. Ma, G. Zheng, *Joule* **2018**, *2*, 1610-1622.
- [4] (a) M.-A. Légaré, G. Bélanger-Chabot, R. D. Dewhurst, E. Welz, I. Krummenacher, B. Engels, H. Braunschweig, *Science* **2018**, *359*, 896-900; (b) M.-A. Légaré, M. Rang, G. Bélanger-Chabot, J. I. Schweizer, I. Krummenacher, R. Bertermann, M. Arrowsmith, M. C. Holthausen, H. Braunschweig, *Science* **2019**, *363*, 1329-1332; (c) M.-A. Légaré, G. Bélanger-Chabot, M. Rang, R. D. Dewhurst, I. Krummenacher, R. Bertermann, H. Braunschweig, *Nat. Chem.* **2020**, *12*, 1076-1080.
- [5] (a) A. M. Rouf, C. Dai, F. Xu, J. Zhu, *Adv. Theory Simul.* **2020**, *3*, 1900205; (b) A. M. Rouf, C. Dai, S. Dong, J. Zhu, *Inorg. Chem.* **2020**, *59*, 11770-11781; (c) A. M. Rouf, Y. Huang, S. Dong, J. Zhu, *Inorg. Chem.* **2021**, *60*, 5598-5606.
- [6] (a) D. Martin, M. Soleilhavoup, G. Bertrand, *Chem. Sci.* **2011**, *2*, 389-399; (b) H. Song, Y. Kim, J. Park, K. Kim, E. Lee, *Synlett* **2016**, *27*, 477-485.
- [7] (a) X. Li, K. Liu, X. Xu, L. Ma, H. Wang, D. Jiang, Q. Zhang, C. Lu, *Chem. Commun.* **2011**, *47*, 7860-7862; (b) J. L. Peltier, E. Tomás-Mendivil, D. R. Tolentino, M. M. Hansmann, R. Jazzar, G. Bertrand, *J. Am. Chem. Soc.* **2020**, *142*, 18336-18340.
- [8] (a) A. J. Arduengo, R. L. Harlow, M. Kline, *J. Am. Chem. Soc.* **1991**, *113*, 361-363; (b) A. J. Arduengo, J. R. Goerlich, W. J. Marshall, *J. Am. Chem. Soc.* **1995**, *117*, 11027-11028; (c) R. W. Alder, M. E. Blake, C. Bortolotti, S. Bufali, C. P. Butts, E. Linehan, J. M. Oliva, A. Guy Orpen, M. J. Quayle, *Chem. Commun.* **1999**, 241-242; (d) D. Martin, N. Lassauque, B. Donnadieu, G. Bertrand, *Angew. Chem. Int. Ed.* **2012**, *51*, 6172-6175; (e) T. W. Hudnall, C. W. Bielawski, *J. Am. Chem. Soc.* **2009**, *131*, 16039-16041; (f) M. Braun, W. Frank, G. J. Reiss, C. Ganter, *Organometallics* **2010**, *29*, 4418-4420; (g) R. W. Alder, P. R. Allen, M. Murray, A. G. Orpen, *Angew. Chem. Int. Ed. Engl.* **1996**, *35*, 1121-1123; (h) A. J. Arduengo III, J. R. Goerlich, W. J. Marshall, *Liebigs Ann.* **1997**, *1997*, 365-374; (i) V. Lavallo, Y. Canac, C. Präsang, B. Donnadieu, G. Bertrand, *Angew. Chem. Int. Ed.* **2005**, *44*, 5705-5709; (j) C. M. Weinstein, G. P. Junor, D. R. Tolentino, R. Jazzar, M. Melaimi, G. Bertrand, *J. Am. Chem. Soc.* **2018**, *140*, 9255-9260; (k) B. Rao, H. Tang, X. Zeng, L. L. Liu, M. Melaimi, G. Bertrand, *Angew. Chem. Int. Ed.* **2015**, *54*, 14915-14919; (l) H. Song, H. Kim, E. Lee, *Angew. Chem. Int. Ed.* **2018**, *57*, 8603-8607; (m) Z. R. McCarty, D. N. Lastovickova, C. W. Bielawski, *Chem. Commun.* **2016**, *52*, 5447-5450; (n) P. R. Sultane, G. Ahumada, D. Janssen-Müller, C. W. Bielawski, *Angew. Chem. Int. Ed.* **2019**, *58*, 16320-16325; (o) M. B. Gildner, T. W. Hudnall, *Chem. Commun.* **2019**, *55*, 12300-12303; (p) V. Lavallo, J. Mafhouz, Y. Canac, B. Donnadieu, W. W. Schoeller, G. Bertrand, *J. Am. Chem. Soc.* **2004**, *126*, 8670-8671; (q) X. Cattoën, H. Gornitzka, D. Bourissou, G. Bertrand, *J. Am. Chem. Soc.* **2004**, *126*, 1342-1343; (r) G. A. Blake, J. P. Moerdyk, C. W. Bielawski, *Organometallics* **2012**, *31*, 3373-3378; (s) H. Kim, M. Kim, H. Song, E. Lee, *Chem. Eur. J.* **2021**, *27*, 3849-3854; (t) R. W. Alder, C. P. Butts, A. G. Orpen, *J. Am. Chem. Soc.* **1998**, *120*, 11526-11527.
- [9] P. L. Holland, *Dalton Trans.* **2010**, *39*, 5415-5425.
- [10] J.-Y. Guo, Y. Minko, C. B. Santiago, M. S. Sigman, *ACS Catal.* **2017**, *7*, 4144-4151.
- [11] (a) S. Solé, H. Gornitzka, W. W. Schoeller, D. Bourissou, G. Bertrand, *Science* **2001**, *292*, 1901-1903; (b) J. Vignolle, M. Asay, K. Miqueu, D. Bourissou, G. Bertrand, *Org. Lett.* **2008**, *10*, 4299-4302; (c) J. Lorkowski, M. Krahuß, M. Kubicki, U. Radius, C. Pietraszuk, *Chem. Eur. J.* **2019**, *25*, 11365-11374.
- [12] M. J. Chalkley, M. W. Drover, J. C. Peters, *Chem. Rev.* **2020**, *120*, 5582-5636.
- [13] G. Knizia, J. E. M. N. Klein, *Angew. Chem. Int. Ed.* **2015**, *54*, 5518-5522